

I Have Covered All the Bases Here: Interpreting Reasoning Features in Large Language Models via Sparse Autoencoders

Andrey Galichin^{1,2,3}, Alexey Dontsov^{1,5},
 Polina Druzhinina^{1,3}, Anton Razzhigaev^{1,3},
 Oleg Y. Rogov^{1,2,3}, Elena Tutubalina^{1,4}, Ivan Oseledets^{1,3}

¹AIRI ²MTUCI ³Skoltech ⁴Sber ⁵HSE

Correspondence: galichin@airi.net; rogov@airi.net

Abstract

Recent LLMs like DEEPSEEK-R1 have demonstrated state-of-the-art performance by integrating deep thinking and complex reasoning during generation. However, the internal mechanisms behind these reasoning processes remain unexplored. We observe *reasoning* LLMs consistently use vocabulary associated with human reasoning processes. We hypothesize these words correspond to specific reasoning moments within the models' internal mechanisms. To test this hypothesis, we employ Sparse Autoencoders (SAEs), a technique for sparse decomposition of neural network activations into human-interpretable features. We introduce *ReasonScore*, an automatic metric to identify active SAE features during these reasoning moments. We perform manual and automatic interpretation of the features detected by our metric, and find those with activation patterns matching uncertainty, exploratory thinking, and reflection. Through steering experiments, we demonstrate that amplifying these features increases performance on reasoning-intensive benchmarks (+2.2%) while producing longer reasoning traces (+20.5%). Using the model diffing technique, we provide evidence that these features are present only in models with reasoning capabilities. Our work provides the first step towards a mechanistic understanding of reasoning in LLMs.¹

1 Introduction

Large Language Models (LLMs) have achieved remarkable success in natural language processing (Brown et al., 2020), evolving beyond simple token prediction tasks towards explicit reasoning behaviors, such as step-by-step problem-solving (Wei et al., 2022; Kojima et al., 2022; Wang et al., 2022) and self-reflection (Madaan et al., 2023; Shinn et al., 2023). Recently, specialized models which we denote as *reasoning* models, such

Problem: Convert the point $(0, 3)$ in rectangular coordinates to polar coordinates. Enter your answer in the form (r, θ) , where $r > 0$ and $0 \leq \theta < 2\pi$.

Generation (no steering): Okay, so I have this problem where I need to convert the rectangular coordinates $(0, 3)$ to polar coordinates. $\{... 1500 \text{ tokens} ... \} \leftarrow \text{Reasoning trace}$
 So, putting it all together, $(0, 3)$ in rectangular coordinates is $(3, \pi/2)$ in polar coordinates.

Generation (steering): Okay, so I have this problem here where I need to convert the point $(0, 3)$ from rectangular (which is the same as Cartesian) coordinates to polar coordinates. $\{... 2000 \text{ tokens} ... \} \leftarrow \text{Increased reasoning trace}$
 $\text{I think I've covered all the bases here.}$
 Calculated r , determined θ , checked using different methods, and even considered the quadrant placement. I don't see any issues with the reasoning. So, I feel confident that the polar coordinates for the point $(0, 3)$ are $(3, \pi/2)$.

Figure 1: Illustration of steering (amplifying) reasoning-specific features during LLM generation. Default generation (blue) shows standard model reasoning, whereas steering (green) induces increased reasoning, self-correction, and graceful transition to the final answer—evidence that the identified features are responsible for the *reasoning* concept.

as OpenAI's o1 (OpenAI, 2024b) and DEEPSEEK-R1 (Guo et al., 2025), have significantly improved performance on complex reasoning tasks. Trained through advanced fine-tuning and reinforcement learning (Shao et al., 2024), these models incorporate reasoning and reflective problem-solving by generating long chains of thought before providing final answers. These advances raise a new research question: How are such reasoning capabilities internally encoded within LLMs?

A growing body of work suggests that LLMs represent meaningful concepts as linear directions in their activation spaces (Mikolov et al., 2013; Elhage et al., 2022; Park et al., 2023; Nanda et al.,

¹Code available at <https://github.com/AIRI-Institute/SAE-Reasoning>

2023; Jiang et al., 2024). However, identifying these directions remains challenging. Sparse Autoencoders (SAEs) offer a principled approach to disentangle activations into sparse, interpretable *features* (Cunningham et al., 2023; Gao et al., 2024b; Templeton, 2024; Marks et al., 2024). Given a trained SAE, the interpretation of its features could be performed by activation analysis (Bricken et al., 2023), targeted interventions (Templeton, 2024), or automated methods (Paulo et al., 2024; Kuznetsov et al., 2025). While SAEs have proven effective in discovering features for various concepts (Shu et al., 2025), their ability to isolate reasoning-specific features remains unexplored.

In this work, we investigate whether reasoning processes in *reasoning* LLMs can be identified and decomposed into interpretable directions within their activation spaces. We analyze the outputs produced by these models’, and find a consistent pattern in which they employ words associated with human reasoning processes: uncertainty (e.g. “perhaps”), reflection (e.g. “however”), and exploration (e.g. “alternatively”) (Chinn and Anderson, 1998; Boyd and Kong, 2017; Gerns and Mortimore, 2025). We hypothesize that these linguistic patterns correspond to the moments of reasoning within the models’ internal mechanisms. To test this, we construct a vocabulary of reasoning words. We then use SAEs to decompose LLM activations into interpretable features and propose ReasonScore, a metric that quantifies the degree to which a given SAE feature is active on the reasoning vocabulary.

We evaluate the features found by ReasonScore using manual (Bricken et al., 2023) and automatic interpretation (Kuznetsov et al., 2025) techniques, and find the set of 46 features that demonstrate interpretable activation patterns corresponding to uncertainty, exploratory thinking, and reflection. We perform steering experiments and show that amplifying these reasoning features leads to improved performance on reasoning-intensive benchmarks (+13.4% on AIME-2024, +2.2% on MATH-500, and +4% on GPQA Diamond) while producing longer reasoning traces (+18.5% on AIME-2024, +20.5% on MATH-500, and +13.9% on GPQA Diamond). Through model diffing (Bricken et al., 2024), we demonstrate that these reasoning features emerge only in *reasoning* LLMs and are absent in base models. Our results provide mechanistic evidence that specific, interpretable components in LLMs representations are causally linked to reasoning behavior.

The contributions of this paper are the following:

- We introduce ReasonScore, an automatic metric to identify the SAE features responsible for reasoning and confirm its effectiveness using interpretability techniques.
- We provide causal evidence from steering experiments, demonstrating that amplifying identified features induces reasoning behavior.
- We analyze the emergence of reasoning features in LLMs through model diffing technique, and confirm their existence only after the *reasoning* fine-tuning stage.

2 Interpretability with SAEs

Sparse Autoencoders (SAEs) aim to learn a sparse decomposition of model activations to identify disentangled features that correspond to meaningful concepts (Bricken et al., 2023). Here, a *feature* refers to an individual component of the learned representation that captures specific, human-interpretable characteristics of the input data.

The core idea behind SAEs is to reconstruct model activations $x \in \mathbb{R}^n$ as a sparse linear combination of learned feature directions, where the feature *dictionary* dimensionality $m \gg n$. Formally, we extract LLM activations from some intermediate state in the model and train a two-layer autoencoder:

$$\begin{aligned} f(x) &= \sigma(W_{\text{enc}}x + b_{\text{enc}}), \\ \hat{x}(f) &= W_{\text{dec}}f + b_{\text{dec}}. \end{aligned} \quad (1)$$

Here, $f(x) \in \mathbb{R}^m$ is a sparse vector of feature magnitudes and $\hat{x}(f) \in \mathbb{R}^n$ is a reconstruction of the original activation x . The columns of W_{dec} , which we denote by $W_{\text{dec},i}$, $i = 1, \dots, m$, represent the dictionary of directions, or *features*, into which the SAE decomposes x . The activation function σ enforces non-negativity in $f(x)$.

The training objective used to train Sparse Autoencoders minimizes a reconstruction loss $\mathcal{L}_{\text{recon}}$ and an additional sparsity-promoting loss $\mathcal{L}_{\text{sparsity}}$. This objective forces SAE to learn a small set of interpretable features that capture the distinct properties of the activations.

In our work, we use vanilla SAE (Bricken et al., 2023) with ReLU activation function. Following (Conerly et al., 2024), we use a squared error reconstruction loss and a modified L1 penalty as a

sparsity loss:

$$\mathcal{L} = \underbrace{\|x - \hat{x}\|_2^2}_{\mathcal{L}_{\text{recon}}} + \lambda \underbrace{\sum_{i=1}^m f_i \|W_{\text{dec},i}\|_2}_{\mathcal{L}_{\text{sparsity}}}, \quad (2)$$

where λ is the sparsity penalty coefficient.

3 Method

We identify reasoning-specific features through a two-step approach. First, we examine the language space of reasoning words used by *reasoning* LLMs, and construct the respective vocabulary \mathcal{R} (Sec. 3.1). Secondly, we introduce ReasonScore to find the sparse autoencoder features responsible for reasoning capabilities (Sec. 3.2).

3.1 Reasoning Vocabulary

Reasoning words are linguistic features associated with exploratory talk as humans talk-to-learn, explore ideas, and probe each other’s thinking (Boyd and Kong, 2017).

In the original DEEPSEEK-R1 paper (Guo et al., 2025), the authors demonstrated that the model spontaneously exhibits sophisticated human-like behaviors, such as reflection, where it revisits and reevaluates its previous steps, and exploration of alternative problem-solving approaches. In particular, the model explicitly employs words that mirror the introspective language humans use when thinking (such as “maybe”, “but”, “wait”). We hypothesize that these moments correspond directly to the internal reasoning process of the models, which is consistent with studies on human thinking (Chinn and Anderson, 1998; Boyd and Kong, 2017).

To extract the models’ reasoning vocabulary, we use an approach similar to that of (Rayson and Garside, 2000). We construct two corpora from the OPENTHOUGHTS-114K (OpenThoughts, 2025) dataset: ground-truth samples containing formal and step-by-step solutions to the problems, and the solutions obtained using DEEPSEEK-R1 for the same problems. For each word, we calculate its frequency in the tasks solutions p_{solution} and in the thinking solutions p_{think} , then sort all words by the frequency difference $p_{\text{think}} - p_{\text{solution}}$. Next, we select the top- k words by frequency difference, where k is determined by the point where the frequency distribution plateaus, and filter out words with high presence in the Google Books Ngram Corpus (Michel et al., 2011) (Fig. 2). To determine the final vocabulary from this candidate set, we choose words that best capture reasoning behavior.

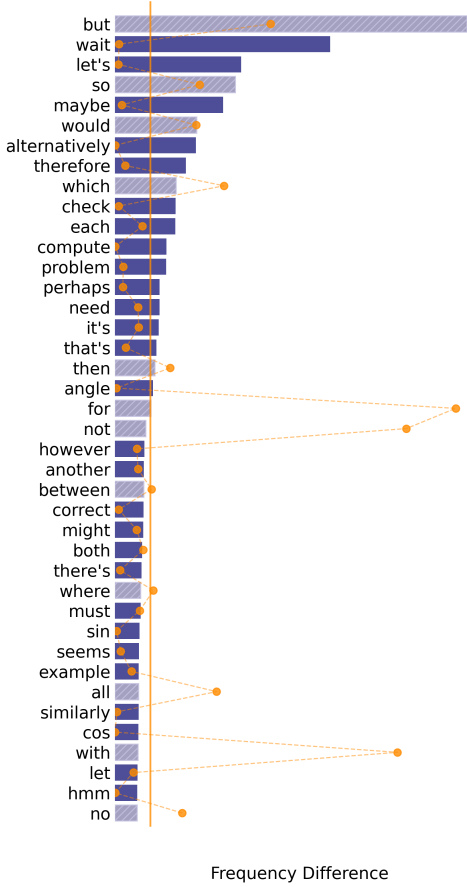


Figure 2: The distribution of top 40 words with the greatest change in frequency between reasoning traces of DEEPSEEK-R1 and ground-truth solutions of math problems. Orange dots show the frequency from Google Books Ngram Corpus. We remove the words with absolute frequency above the pre-defined threshold (orange line), and keep those with the high relative frequency indicating reasoning.

This includes words that match those considered in the linguistic literature (Chinn and Anderson, 1998; Boyd and Kong, 2017) and those that we identify through manual analysis of model traces exhibiting reasoning patterns.

Following this pipeline, we select 10 words indicating reasoning as models’ *reasoning* vocabulary and denote it by \mathcal{R} . The exact list of words can be found in Appx. A.1. Ablation experiments confirm that these words play a functional role in reasoning capabilities (see Sec. 4.3 for setup, Appx. A.2 for results).

3.2 ReasonScore

To find SAE features that capture reasoning-related behavior, we follow our hypothesis and introduce ReasonScore, which measures the contribution

```

Feature #4395
But how to verify this.\n\nLet me re-express
the inequalities hold. But wait, maybe the constant c
up to some equivalence.\n\nBut let me check if there
So this is unclear.\n\nBut looking at the sample

Feature #25953
rahedra.\n\nWait, here's another idea.

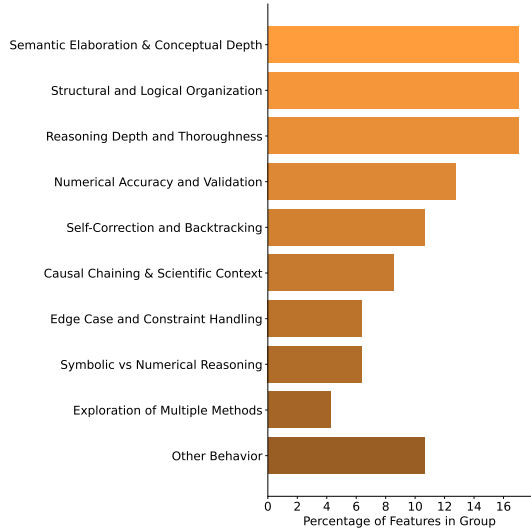
(71 pm). Wait, maybe different sources have slightly
formula has a different sign.\n\nAlternatively, maybe the
coefficient low. Let me verify. Another way: I remember

Feature #46691
mass ranges. Hmm.\n\nNow, detection. LIGO
the starting points. That seems a bit counterintuitive
trigonometric identities. Hmm, but maybe a synthetic
regardless of starting values. Interesting.\n\nLet me try to

Feature #61104
some code?), but that's not standard. Alternatively,
is in a different row. That doesn't make sense
That's a stretch, but perhaps that's the connection
, then maybe more. Wait, this is getting complicated

```

(a) Top-activating examples from the manually verified set of features.



(b) Distribution of manually verified set of features on function groups generated by GPT-4O.

Figure 3: Interpretability results for manually verified set of features in our SAE: (a) Examples of feature interfaces used in manual interpretation experiments, (b) Distribution of reasoning features on function groups obtained by automatic interpretation pipeline by using GPT-4O as a judge.

of i -th feature to reasoning. Using a dataset of model’s activations (see details in Sec. 4.1) $\mathcal{D} = \mathcal{D}_{\mathcal{R}} \cup \mathcal{D}_{\neg\mathcal{R}}$, where $\mathcal{D}_{\mathcal{R}}$ contains token activations corresponding to words in \mathcal{R} and $\mathcal{D}_{\neg\mathcal{R}}$ contains all other activations, we first define a score:

$$s_i = \frac{\mu(i, \mathcal{D}_{\mathcal{R}})}{\sum_j \mu(j, \mathcal{D}_{\mathcal{R}})} - \frac{\mu(i, \mathcal{D}_{\neg\mathcal{R}})}{\sum_j \mu(j, \mathcal{D}_{\neg\mathcal{R}})}, \quad (3)$$

where $\mu(i, \mathcal{D}) = \frac{1}{|\mathcal{D}|} \sum_{x \in \mathcal{D}} f_i(x)$ is the average activation value of the i -th feature on dataset \mathcal{D} . This score is similar to the one in (Cywiński and Deja, 2025) and identifies features that concentrate the most of their activation mass on reasoning words.

However, analysis of feature activations only on individual words may miss important contextual information. The words in \mathcal{R} are critical indicators of the reasoning process and also serve as transition points, signaling shifts in the thought process, uncertainty, or reflection. Therefore, a feature involved in reasoning should activate not only on the reasoning words, but also as the model approaches and continues through these transitions. To capture it, we define $\mathcal{D}_{\mathcal{R}}^W$ as the dataset that contains activations within a fixed-width context window around tokens corresponding to words in \mathcal{R} , and $\mathcal{D}_{\neg\mathcal{R}}^W$ contains all other activations. We modify Eq. 3 to use the new version of the datasets.

To penalize features that activate only on a small fraction of \mathcal{R} , we further introduce an *en-*

tropy penalty. For i -th feature, we first calculate $\mu(i, \mathcal{D}_{r_j}^W)$ for each word $r_j \in \mathcal{R}$, normalize these values into a probability distribution $p_i(r_j) = \frac{\mu(i, \mathcal{D}_{r_j}^W)}{\sum_{k \in \mathcal{R}} \mu(i, \mathcal{D}_{r_k}^W)}$, and compute the entropy:

$$H_i = -\frac{1}{\log |\mathcal{R}|} \cdot \sum_j p_i(r_j) \log p_i(r_j). \quad (4)$$

Here, $\log |\mathcal{R}|$ normalizes the entropy to $[0, 1]$, with $H_i = 1$ indicating perfect uniformity over \mathcal{R} . By adding the entropy penalty in Eq. (3), we define the ReasonScore for the i -th SAE feature as:

$$\text{ReasonScore}_i = \frac{\mu(i, \mathcal{D}_{\mathcal{R}}^W)}{\sum_j \mu(j, \mathcal{D}_{\mathcal{R}}^W)} \cdot H_i^\alpha - \frac{\mu(i, \mathcal{D}_{\neg\mathcal{R}}^W)}{\sum_j \mu(j, \mathcal{D}_{\neg\mathcal{R}}^W)}. \quad (5)$$

where α controls the trade-off between specificity ($\alpha \rightarrow 0$) and generalization ($\alpha > 1$).

We identify the set of reasoning features in a SAE based on their ReasonScore and define the corresponding set of feature indices as:

$$\mathcal{F}_{\mathcal{R}} = \{i \mid i \in [1, m], \text{ReasonScore}_i > \tau\}, \quad (6)$$

where τ is the q -th quantile of the ReasonScore distribution across all features.

4 Evaluation

In this section, we analyze how effectively our discovered features model reflection, uncertainty, and exploration within the *reasoning* model. We discuss our experimental setup (Sec. 4.1), perform manual and automatic interpretation of the features we find (Sec. 4.2), and conduct steering experiments with these features on various benchmarks (Sec. 4.3). Finally, we apply the model diffing technique to demonstrate that these features exist only in models with reasoning capabilities (Sec. 4.4).

4.1 Experimental Setup

Model. We apply SAE to the output activations from the 19-th layer of the DEEPSEEK-R1-LLAMA-8B model. This model was selected for its *reasoning* capabilities and open-source availability. The 19-th layer ($\approx 60\%$ model depth) was chosen because at this point LLMs predominately store the most of their knowledge (Chen et al., 2023; Jin et al., 2024). We provide results for other layers of DEEPSEEK-R1-LLAMA-8B and another model family in Appx. D.

Data. We train SAE on the activations of the model generated using text data from the LMSYS-CHAT-1M (Zheng et al., 2023) and OPENTHOUGHTS-114K (OpenThoughts, 2025) datasets. The first provides a broad and diverse spectrum of real-world text data, which we denote as *base data*, while the latter provides high-quality reasoning traces generated by DEEPSEEK-R1 for math, science, code, and puzzle samples, which we denote as *reasoning data*. The SAE is trained on 1B tokens, evenly split between the two datasets, with a context window of 1,024 tokens.

Training. We set the SAE dictionary dimensionality to $m = 65,536$, which is 16 times larger than the model activation size $n = 4,096$ following established practices (Lieberum et al., 2024), and adopt the same training settings as in the Anthropic April update (Conerly et al., 2024). We train with the Adam optimizer (Kingma and Ba, 2014) with $(\beta_1, \beta_2) = (0.9, 0.999)$, batch size of 4,096, and a learning rate $\eta = 5 \times 10^{-5}$. The learning rate is decayed linearly to zero over the last 20% of training. The gradient norm is clipped to 1. We use a linear warmup for the sparsity coefficient from $\lambda = 0$ to $\lambda = 5$ over the first 5% training steps.

Evaluation. We use the mean L0-norm of latent activations, $\mathbb{E}_x \|f(x)\|_0$, as a measure of sparsity.

Feature #	AIME 2024		MATH-500		GPQA Diamond	
	maj@4	tokens (K)	maj@4	tokens (K)	maj@4	tokens (K)
No steering	53.3	12.4	93.2	3.9	50.0	7.9
3942	56.7	11.1	93.0	3.4	46.5	6.7
4395	56.7	14.7	95.4	4.1	52.0	8.5
16441	60.0	14.0	95.0	4.1	54.0	8.3
16778	56.7	14.1	94.0	4.7	51.0	9.0
25953	60.0	12.8	94.2	4.2	53.0	8.1
46691	56.7	14.0	94.2	4.2	54.0	8.0
61104	66.7	12.0	95.0	3.6	53.0	7.5

Table 1: Performance and average number of output tokens for different steering experiments on reasoning-related benchmarks.

To measure reconstruction quality, we use fraction of variance of the input explained by the reconstruction. Both metrics were computed on 2,048 sequences of length 1,024.

At a L0 of 86 the reconstruction of our SAE explains 68.5% of the variance in model activations. This shows that our SAE achieves reliable reconstruction performance at a low sparsity level, allowing a decomposition of raw activations into interpretable features.

ReasonScore. We calculate ReasonScore (Eq. 5) on 10M tokens from the OPENTHOUGHTS-114K dataset. To collect $\mathcal{D}_{\mathcal{R}}^W$, we use an asymmetric window with 2 preceding and 3 subsequent tokens, following established practices in Keyphrase extraction (Mihalcea and Tarau, 2004; Breidt, 1996; Zhang et al., 2020). We set $\alpha = 0.7$ for the *entropy penalty* as a reasonable default. Based on the empirical analysis of ReasonScore distribution (see Appx. A.3), we set $q = 0.997$ in Eq. (6), resulting in $|\mathcal{F}_{\mathcal{R}}| = 200$ features.

4.2 Interpretability of Reasoning Features

Manual Interpretation. To evaluate the features we found with ReasonScore, we manually interpret each feature from $\mathcal{F}_{\mathcal{R}}$ (200 in total). For each feature, we find the examples in a subset of the OPENTHOUGHTS-114K corpus that caused the feature to activate, and construct the interface proposed in (Bricken et al., 2023). This mainly includes examples of when the feature activates, its effect on the logits when it does, and other statistics. We determine whether a feature qualifies as a good reasoning candidate if: (1) when it is active, the relevant concept is reliably present in the context, (2) it triggers in various examples of reasoning tasks, and (3) its activation impacts interpretable logits that correspond to reasoning processes.

Through our analysis, we identify three behavioral modes that characterize models’ reasoning process:

- **Uncertainty:** Moments where the model exhibits hesitation, doubts, and provisional thinking
- **Exploration:** Moments where the model considers multiple possibilities, connects ideas, examines different perspectives
- **Reflection:** Moments where the model revisits and reevaluates its previous steps

Our manual analysis reveals a set of 46 features that exhibit these patterns, which we believe are responsible for the reasoning mechanisms of the model. We denote this set by $\mathcal{F}_{\mathcal{R}}^{\text{manual}} \subset \mathcal{F}_{\mathcal{R}}$. In Fig. 3a, we provide examples of feature interfaces used for interpretation. The results demonstrate features that consistently activate in contexts representing model’s uncertainty (#61104), exploration (#25953), and reflection (#4395, #46691). Additional examples of interfaces can be found in Appx. B.1.

Automatic Interpretation. To complement our manual analysis, we annotate these features with an automatic interpretation pipeline (Kuznetsov et al., 2025). This approach employs feature steering, a technique that modulates feature activations to analyze their functional influence. For each i -th feature, we estimate its maximum activation f_i^{\max} using a subset of the OPENTHOUGHTS-114K corpus. During response generation, we modify model activations as follows:

$$x' = x + \gamma f_i^{\max} W_{\text{dec},i}, \quad (7)$$

where γ controls the steering strength.

To evaluate the impact of i -th feature on reasoning capabilities, we generate multiple outputs by varying $\gamma \in [-4, 4]$, pass them to GPT-4O, and ask it to generate an explanation or function that best describes the semantic influence caused by steering a feature. The result, shown in Fig. 3b, reveals that the features we found group into distinct reasoning-related patterns. Only a small fraction of features from $\mathcal{F}_{\mathcal{R}}^{\text{manual}}$ (5) was assigned to a mixed class “Other Behavior” containing mixed explanation. We provide a more comprehensive description of auto-interpretability pipeline results in Appx. B.2.

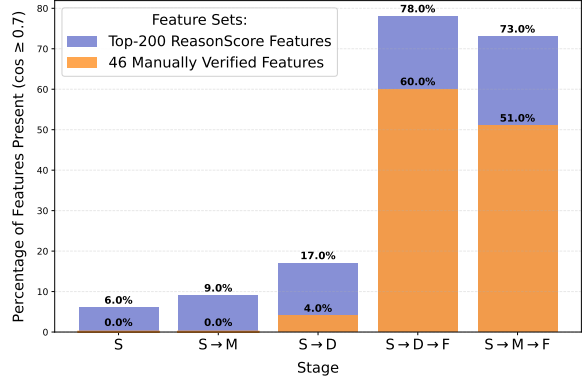


Figure 4: Percentage of ReasonScore features present at each stage of the diffing pipeline. The blue bars represent the features from $\mathcal{F}_{\mathcal{R}}$, the orange bars represent the $\mathcal{F}_{\mathcal{R}}^{\text{manual}}$ features. Features are considered present if their cosine similarity with any feature in corresponding stage’s SAE is ≥ 0.7 . Stages: (S) Base model + base data; (S → D) Base model + reasoning data; S → M Reasoning model + base data; (S → D/M → F) Reasoning model + reasoning data.

Takeaway 1: Manual interpretation experiments confirm that ReasonScore identifies features that describe model’s reasoning capabilities, revealing 46 features that represent uncertainty, exploration, and reflection. Automatic interpretation demonstrates that these features are causally linked to reasoning behavior.

4.3 Steering Reasoning Features

To demonstrate whether our interpretations of features describe their influence on model behavior, we further experiment with feature steering.

Our goal is to verify if steering reasoning features improve the LLM’s performance on reasoning-related benchmarks. Following the setup in DEEPSEEK-R1, we evaluate performance on AIMIE 2024 (of America, 2024), MATH-500 (Hendrycks et al., 2021), and GPQA Diamond (Rein et al., 2023). To obtain steering results for i -th feature, we modify the activations during response generation according to Eq. (7). To determine the optimal steering strength that can influence model outputs without significantly damaging capabilities, we ran evaluations with a small subset of 10 reasoning features on MATH-500. We varied the steering strength γ from 1 to 8. Based on these experiments, we determined the optimal range $\gamma \in [1, 3]$, which aligns with the findings in (Durmus et al., 2024). For all subsequent experi-

ments, we set the steering strength $\gamma = 2$.

We perform a preliminary analysis to identify the most promising features for reasoning enhancement from our set of manually chosen features $\mathcal{F}_{\mathcal{R}}^{\text{manual}}$. For each feature, we measure the accuracy (or $\text{pass}@1$ (Chen et al., 2021)) on MATH-500 and evaluate the results. Of the 46 features, 9 improve performance by $\geq 0.5\%$, 29 show no or minimal performance degradation ($\leq 2.0\%$), and the remaining 8 decrease performance by at most 4%. Interestingly, we identify feature #3942, which produces substantially shorter responses while maintaining negligible performance degradation. For further analysis, we select the 9 top-performing features and feature #3942.

We evaluate these 10 features across all reasoning benchmarks. We report $\text{maj}@4$ ((Wang et al., 2022; Muennighoff et al., 2025)) and the average number of tokens generated during the model’s thinking process. The results, shown in Tab. 1, demonstrate that steering 7 out of 10 features produces consistent improvements in both performance and reasoning depth. Feature #4395 yields the most significant performance gain on MATH-500 (+2.2%). Feature #16778 produces the longest reasoning traces on average (+13.7% on AIME-2024, +20.5% on MATH-500, and +13.9% on GPQA Diamond) and consistently outperforms the “no steering” baseline. Feature #3942 produces shortest reasoning traces on average (-7.7%) with minor performance degradation. We provide examples of generated solutions without and with feature steering in Appx. C.

Takeaway 2: We find that amplifying certain reasoning features prolongs the internal thought process and correlates with increased performance on reasoning-related tasks.

4.4 Stage-wise Emergence of Reasoning Features

Our interpretation experiments (Sec. 4.2) revealed that features identified by ReasonScore exhibit activation patterns consistent with reasoning processes. The steering experiments (Sec. 4.3) provided causal evidence by demonstrating that amplification of these features improves performance on reasoning-intensive benchmarks. Given these findings, we now aim to answer the next important question: do these reasoning features naturally

emerge during standard pre-training procedure, or are they specifically induced by the *reasoning* fine-tuning process?

To answer this question, we use the stage-wise fine-tuning technique proposed in (Bricken et al., 2024). This approach aims to isolate how features evolve across different model and dataset combinations. In our experiments, we examine how the features change between two model states: before (*base model*) and after (*reasoning model*) *reasoning* fine-tuning stage. We accomplish this by training a SAE on the base model before it has been fine-tuned, and then fine-tuning it on either the reasoning model or the fine-tuning data. Formally, we define four distinct stages:

Stage S: base model + base data (starting point)

Stage D: base model + reasoning data (isolating dataset effects)

Stage M: reasoning model + base data (isolating model effects)

Stage F: reasoning model + reasoning data (full fine-tuning)

We analyze these changes through two fine-tuning trajectories, each involving two sequential fine-tuning stages: (1) **S**→**D**→**F** takes initial SAE (Stage S), fine-tunes it on reasoning data (**S**→**D**), and finally fine-tunes on both reasoning model and reasoning data (**D**→**F**); (2) **S**→**M**→**F** takes initial SAE (Stage S), fine-tunes it on reasoning model (**S**→**M**), and finally fine-tunes on both reasoning model and reasoning data (**M**→**F**). If reasoning features are present only in *reasoning* models, we should observe the emergence of these features in response to **both** reasoning model and reasoning data (Stage F). This corresponds to the final steps of the fine-tuning trajectories: (**S**→**D**/**M**→**F**).

We use LLAMA-3.1-8B (Grattafiori et al., 2024) as base model and SLIMPAJAMA (Soboleva et al., 2023) as base data. We select SLIMPAJAMA over LMSYS-CHAT-1M as our *base data* because it better matches the pre-training distribution of LLAMA-3.1-8B, which has not undergone instruction-tuning. For each stage, we use the same setup as in Sec. 4.1, with each fine-tuning stage taking 30% of the total number of tokens required for training from scratch. For each i -th feature from $\mathcal{F}_{\mathcal{R}}$, we check its existence at each stage by measuring cosine similarity (cos) between feature vectors. We follow (Bricken et al., 2024) and consider a feature

present if $\cos \geq 0.7$ with any feature in a SAE of the corresponding stage.

Fig. 4 shows the percentage of reasoning features present at each fine-tuning stage. We find that the reasoning features are almost absent in the base model and after switching to the reasoning model (0% of manually verified features $\mathcal{F}_R^{\text{manual}}$). When introducing the reasoning data to the base model ($\mathbf{S} \rightarrow \mathbf{D}$), only 4% of the verified reasoning features emerge, indicating that exposure to the reasoning content alone is insufficient to develop these features. Finally, when we incorporate both the reasoning data and the reasoning model, we observe that 60% of the verified reasoning features appear in the ($\mathbf{S} \rightarrow \mathbf{D} \rightarrow \mathbf{F}$) stage and 51% in the ($\mathbf{S} \rightarrow \mathbf{M} \rightarrow \mathbf{F}$) stage. The noticeable increase in the presence of features only when both reasoning data and model are combined provides compelling evidence that ReasonScore identifies features associated with the model’s reasoning processes rather than general capabilities.

Takeaway 3: We show that most of the features found by ReasonScore emerge only after the *reasoning* fine-tuning stage. Exposure to the reasoning data or reasoning model alone is insufficient to develop these features.

5 Related Work

5.1 Mechanistic Interpretability

Various methods exist to shed light on the inner workings of LLMs, including attention analysis, which examines the model’s focus on input tokens (Vaswani et al., 2017), and gradient-based methods that identify influential input features (Simonyan et al., 2014). Probing techniques offer insights into the information captured within different layers of an LLM (Alain and Bengio, 2016). Mechanistic interpretability aims to reverse-engineer the computations of LLMs, employing techniques like activation patching (Meng et al., 2022) and feature steering (Cao et al., 2024; Soo et al., 2025) to understand and control model behavior. The logit lens provides a way to observe the model’s token predictions at different processing stages (NostalgiaBraist, 2020).

5.2 Sparse Autoencoders

SAEs have emerged as a key tool for understanding the internal representations of LLMs in in-

terpretability research (Gao et al., 2024a; Huben et al., 2024). By learning a sparse decomposition of model activations, SAEs identify disentangled features that correspond to meaningful concepts (Marks et al., 2024).

SAE features are significantly more monosemantic than individual neurons, making them effective for mechanistic interpretability (Leask et al., 2025). A key challenge in using SAEs for interpretability is ensuring that the extracted features are monosemantic and robust. Yan et al. (Yan et al., 2024) propose using feature decorrelation losses to enforce better separation between learned latents, preventing redundancy. Recent advances in cross-layer SAEs (Shi et al., 2025) enable the analysis of more abstract, high-level reasoning patterns across multiple layers.

SAEs have proven valuable for studying model development across training stages. Crosscoders (Lindsey et al., 2024) enable direct feature mapping to model states, while stage-wise model diffing (Bricken et al., 2024) compares SAEs trained on different checkpoints. We adopt the diffing approach for its computational efficiency and intuitive implementation. While previous work has applied diffing to sleeper agents, our research extends this approach to investigate reasoning behavior.

5.3 Reasoning LLMs

Recent LLM innovations have focused on models with explicit reasoning abilities, including OpenAI’s o1 (OpenAI, 2024b), DEEPSEEK-R1 (Guo et al., 2025), and QWQ-32B-PREVIEW (Team, 2024). These methods employ rule-based reinforcement learning using correctness scores (final answer accuracy) and format scores (output structure compliance), leading to advanced reasoning behaviors like self-correction and reflection, denoted as an “aha moment” in the DEEPSEEK-AI report (Guo et al., 2025).

Despite the success of rule-based reinforcement learning in enabling reasoning capabilities, how these models encode their internal reasoning remains unclear. We address this problem using SAEs to find interpretable features responsible for underlying reasoning mechanisms, which, to the best of our knowledge, has not been done yet.

6 Conclusion

In this work, we present a novel methodology for uncovering reasoning mechanisms in LLMs

through SAEs. We introduce ReasonScore, a metric that identifies reasoning-related SAE features based on their activation patterns using a curated introspective vocabulary. Manual and automatic interpretation reveal features corresponding to uncertainty, exploratory thinking, and self-reflection. Through steering experiments, we provide causal evidence that certain features selected by ReasonScore directly correspond to the model’s reasoning behaviors. Amplifying them prolongs the internal thought process and increases performance on reasoning-related benchmarks. Stage-wise analysis confirms that these features emerge only after reasoning fine-tuning. Our work provides the first mechanistic evidence that specific, interpretable components of LLM representations are causally linked to complex reasoning behaviors.

Limitations

ReasonScore. Our metric depends on hyperparameters (window size, entropy penalty α) that require further ablation studies. Of the 200 candidates, we found 46 interpretable features. Although other features can also contribute to reasoning, we could not confidently classify them due to ambiguous activation patterns. Finally, our reasoning vocabulary may not capture all reasoning patterns. These limitations suggest opportunities for future work.

SAEs. SAEs provide a powerful interpretability framework. However, it suffers from problems that complicate the extraction of fully interpretable features (Chanin et al., 2024; Leask et al., 2025). This may cause us to miss some features.

Emergence of Reasoning Features. Although the results in Sec. 4.4 support our hypothesis, we acknowledge certain limitations of the diffing approach. The cosine similarity threshold (0.7) is empirically chosen following the initial work, and may miss similar features if the representation is rotated during one of the fine-tuning stages. Only 60% of the verified features (and 78% of the \mathcal{F}_R features) appeared in the final stage, likely due to fine-tuning SAE rather than training from scratch. These limitations show that our approach can result in false negative and false positive predictions. However, we believe that our primary finding remains valid even under these limitations.

References

Guillaume Alain and Yoshua Bengio. 2016. Understanding intermediate layers using linear classifier probes. *arXiv preprint arXiv:1610.01644*.

Nikita Balagansky, Ian Maksimov, and Daniil Gavrilov. 2024. Mechanistic permutability: Match features across layers. *arXiv preprint arXiv:2410.07656*.

Akhiad Bercovich, Itay Levy, Izik Golan, Mohammad Dabbah, Ran El-Yaniv, Omri Puny, Ido Galil, Zach Moshe, Tomer Ronen, Najeeb Nabwani, and 1 others. 2025. Llama-nemotron: Efficient reasoning models. *arXiv preprint arXiv:2505.00949*.

Maureen Boyd and Yiren Kong. 2017. Reasoning words as linguistic features of exploratory talk: Classroom use and what it can tell us. *Discourse Processes*, 54(1):62–81.

Elisabeth Breidt. 1996. Extraction of vn-collocations from text corpora: A feasibility study for german. *arXiv preprint cmp-lg/9603006*.

Trenton Bricken, Siddharth Mishra-Sharma, Jonathan Marcus, Adam Jermyn, Christopher Olah, Kelley Rivoire, and Thomas Henighan. 2024. Stage-wise model diffing. *Transformer Circuits Thread*.

Trenton Bricken, Adly Templeton, Joshua Batson, Brian Chen, Adam Jermyn, Tom Conerly, Nick Turner, Cem Anil, Carson Denison, Amanda Askell, and 1 others. 2023. Towards monosemanticity: Decomposing language models with dictionary learning, 2023. URL <https://transformer-circuits.pub/2023/monosemantic-features/index.html>, page 9.

Tom Brown, Benjamin Mann, Nick Ryder, Melanie Subbiah, Jared D Kaplan, Prafulla Dhariwal, Arvind Neelakantan, Pranav Shyam, Girish Sastry, Amanda Askell, and 1 others. 2020. Language models are few-shot learners. *Advances in neural information processing systems*, 33:1877–1901.

Yuanpu Cao, Tianrong Zhang, Bochuan Cao, Ziyi Yin, Lu Lin, Fenglong Ma, and Jinghui Chen. 2024. Personalized steering of large language models: Versatile steering vectors through bi-directional preference optimization. *arXiv preprint arXiv:2406.00045*.

David Chanin, James Wilken-Smith, Tomáš Dulka, Hardik Bhatnagar, and Joseph Bloom. 2024. A is for absorption: Studying feature splitting and absorption in sparse autoencoders. *arXiv preprint arXiv:2409.14507*.

Mark Chen, Jerry Tworek, Heewoo Jun, Qiming Yuan, Henrique Ponde De Oliveira Pinto, Jared Kaplan, Harri Edwards, Yuri Burda, Nicholas Joseph, Greg Brockman, and 1 others. 2021. Evaluating large language models trained on code. *arXiv preprint arXiv:2107.03374*.

Nuo Chen, Ning Wu, Shining Liang, Ming Gong, Linjun Shou, Dongmei Zhang, and Jia Li. 2023. Beyond surface: Probing llama across scales and layers. *arXiv preprint arXiv:2312.04333*.

Clark A. Chinn and Richard C. Anderson. 1998. The structure of discussions that promote reasoning. *Teachers College Record*, 100(2):315–368.

Tom Conerly, Adly Templeton, Trenton Bricken, Jonathan Marcus, and Tom Henighan. 2024. Update on how we train saes. *Transformer Circuits Thread*.

Hoagy Cunningham, Aidan Ewart, Logan Riggs, Robert Huben, and Lee Sharkey. 2023. Sparse autoencoders find highly interpretable features in language models. *Preprint*, arXiv:2309.08600.

Bartosz Cywiński and Kamil Deja. 2025. Saeuron: Interpretable concept unlearning in diffusion models with sparse autoencoders. *arXiv preprint arXiv:2501.18052*.

Esin Durmus, Alex Tamkin, Jack Clark, Jerry Wei, Jonathan Marcus, Joshua Batson, Kunal Handa, Liane Lovitt, Meg Tong, Miles McCain, and 1 others. 2024. Evaluating feature steering: A case study in mitigating social biases, 2024. URL <https://anthropic.com/research/evaluating-feature-steering>.

Nelson Elhage, Tristan Hume, Catherine Olsson, Nicholas Schiefer, Tom Henighan, Shauna Kravec, Zac Hatfield-Dodds, Robert Lasenby, Dawn Drain, Carol Chen, and 1 others. 2022. Toy models of superposition. *arXiv preprint arXiv:2209.10652*.

Leo Gao, Tom Dupré la Tour, Henk Tillman, Gabriel Goh, Rajan Troll, Alec Radford, Ilya Sutskever, Jan Leike, and Jeffrey Wu. 2024a. Scaling and evaluating sparse autoencoders. *arXiv preprint arXiv:2406.04093*.

Leo Gao, Tom Dupré la Tour, Henk Tillman, Gabriel Goh, Rajan Troll, Alec Radford, Ilya Sutskever, Jan Leike, and Jeffrey Wu. 2024b. *Scaling and evaluating sparse autoencoders*. *Preprint*, arXiv:2406.04093.

Pilar Gerns and Louisa Mortimore. 2025. Towards exploratory talk in secondary-school clil: An empirical study of the cognitive discourse function ‘explore’. *Language Teaching Research*.

Aaron Grattafiori, Abhimanyu Dubey, Abhinav Jauhri, Abhinav Pandey, Abhishek Kadian, Ahmad Al-Dahle, Aiesha Letman, Akhil Mathur, Alan Schelten, Alex Vaughan, and 1 others. 2024. The llama 3 herd of models. *arXiv preprint arXiv:2407.21783*.

Daya Guo, Dejian Yang, Haowei Zhang, Junxiao Song, Ruoyu Zhang, Runxin Xu, Qihao Zhu, Shirong Ma, Peiyi Wang, Xiao Bi, and 1 others. 2025. Deepseek-r1: Incentivizing reasoning capability in llms via reinforcement learning. *arXiv preprint arXiv:2501.12948*.

Dan Hendrycks, Collin Burns, Saurav Kadavath, Akul Arora, Steven Basart, Eric Tang, Dawn Song, and Jacob Steinhardt. 2021. *Measuring mathematical problem solving with the math dataset*. *Preprint*, arXiv:2103.03874.

Robert Huben, Hoagy Cunningham, Logan R. Smith, Aidan Ewart, and Lee Sharkey. 2024. Sparse autoencoders find highly interpretable features in language models. In *Proceedings of the International Conference on Learning Representations (ICLR)*.

Yibo Jiang, Goutham Rajendran, Pradeep Ravikumar, Bryon Aragam, and Victor Veitch. 2024. On the origins of linear representations in large language models. *arXiv preprint arXiv:2403.03867*.

Mingyu Jin, Qinkai Yu, Jingyuan Huang, Qingcheng Zeng, Zhenting Wang, Wenyue Hua, Haiyan Zhao, Kai Mei, Yanda Meng, Kaize Ding, and 1 others. 2024. Exploring concept depth: How large language models acquire knowledge and concept at different layers? *arXiv preprint arXiv:2404.07066*.

Diederik P Kingma and Jimmy Ba. 2014. Adam: A method for stochastic optimization. *arXiv preprint arXiv:1412.6980*.

Takeshi Kojima, Shixiang Shane Gu, Machel Reid, Yutaka Matsuo, and Yusuke Iwasawa. 2022. Large language models are zero-shot reasoners. *Advances in neural information processing systems*, 35:22199–22213.

Kristian Kuznetsov, Laida Kushnareva, Polina Druzhinina, Anton Razzhigaev, Anastasia Voznyuk, Irina Piontkovskaya, Evgeny Burnaev, and Serguei Baranikov. 2025. Feature-level insights into artificial text detection with sparse autoencoders. *arXiv preprint arXiv:2503.03601*.

Patrick Leask, Bart Bussmann, Michael T. Pearce, Joseph I. Bloom, Curt Tigges, Noura Al Moubayed, Lee Sharkey, and Neel Nanda. 2025. Sparse autoencoders do not find canonical units of analysis. In *Proceedings of the International Conference on Learning Representations (ICLR)*.

Tom Lieberum, Senthooran Rajamanoharan, Arthur Conmy, Lewis Smith, Nicolas Sonnerat, Vikrant Varma, János Kramár, Anca Dragan, Rohin Shah, and Neel Nanda. 2024. Gemma scope: Open sparse autoencoders everywhere all at once on gemma 2. *arXiv preprint arXiv:2408.05147*.

Jack Lindsey, Adly Templeton, Jonathan Marcus, Thomas Conerly, Joshua Batson, and Christopher Olah. 2024. Sparse crosscoders for cross-layer features and model diffing. *Transformer Circuits Thread*.

Aman Madaan, Niket Tandon, Prakhar Gupta, Skyler Hallinan, Luyu Gao, Sarah Wiegreffe, Uri Alon, Nouha Dziri, Shrimai Prabhumoye, Yiming Yang, and 1 others. 2023. Self-refine: Iterative refinement with self-feedback. *Advances in Neural Information Processing Systems*, 36:46534–46594.

Samuel Marks, Can Rager, Eric J Michaud, Yonatan Belinkov, David Bau, and Aaron Mueller. 2024. Sparse feature circuits: Discovering and editing interpretable causal graphs in language models. *arXiv preprint arXiv:2403.19647*.

Kevin Meng, David Bau, Alex Andonian, and Yonatan Belinkov. 2022. Locating and editing factual associations in gpt. In *Advances in Neural Information Processing Systems*.

Jean-Baptiste Michel, Yuan Kui Shen, Aviva Presser Aiden, Adrian Veres, Matthew K Gray, Google Books Team, Joseph P Pickett, Dale Hoiberg, Dan Clancy, Peter Norvig, and 1 others. 2011. Quantitative analysis of culture using millions of digitized books. *science*, 331(6014):176–182.

Rada Mihalcea and Paul Tarau. 2004. Textrank: Bringing order into text. In *Proceedings of the 2004 conference on empirical methods in natural language processing*, pages 404–411.

Tomas Mikolov, Kai Chen, Greg Corrado, and Jeffrey Dean. 2013. Efficient estimation of word representations in vector space. *arXiv preprint arXiv:1301.3781*.

Niklas Muennighoff, Zitong Yang, Weijia Shi, Xiang Li, Li Fei-Fei, Hannaneh Hajishirzi, Luke Zettlemoyer, Percy Liang, Emmanuel Candès, and Tatsunori Hashimoto. 2025. s1: Simple test-time scaling. *arXiv preprint arXiv:2501.19393*.

Neel Nanda, Andrew Lee, and Martin Wattenberg. 2023. Emergent linear representations in world models of self-supervised sequence models. In *Proceedings of the 6th BlackboxNLP Workshop: Analyzing and Interpreting Neural Networks for NLP*, pages 16–30.

Nostalgiaist. 2020. *Interpreting gpt: the logit lens*.

Mathematical Association of America. 2024. *Aime*.

OpenAI. 2024b. Learning to reason with llms. <https://openai.com/index/learning-to-reason-with-llms/>.

OpenThoughts. 2025. Open Thoughts. <https://openthoughts.ai>.

Kiho Park, Yo Joong Choe, and Victor Veitch. 2023. The linear representation hypothesis and the geometry of large language models. *arXiv preprint arXiv:2311.03658*.

Gonçalo Paulo, Alex Mallen, Caden Juang, and Nora Belrose. 2024. Automatically interpreting millions of features in large language models. *arXiv preprint arXiv:2410.13928*.

Paul Rayson and Roger Garside. 2000. *Comparing corpora using frequency profiling*. In *Proceedings of the Workshop on Comparing Corpora - Volume 9*, WCC '00, pages 1–6, USA. Association for Computational Linguistics.

David Rein, Betty Li Hou, Asa Cooper Stickland, Jackson Petty, Richard Yuanzhe Pang, Julien Diranji, Julian Michael, and Samuel R. Bowman. 2023. *Gpqa: A graduate-level google-proof q&a benchmark*. *Preprint*, arXiv:2311.12022.

Zhihong Shao, Peiyi Wang, Qihao Zhu, Runxin Xu, Junxiao Song, Xiao Bi, Haowei Zhang, Mingchuan Zhang, YK Li, Y Wu, and 1 others. 2024. Deepseekmath: Pushing the limits of mathematical reasoning in open language models. *arXiv preprint arXiv:2402.03300*.

Wei Shi, Sihang Li, Tao Liang, Mingyang Wan, Guojun Ma, Xiang Wang, and Xiangnan He. 2025. Route sparse autoencoder to interpret large language models. *arXiv preprint arXiv:2503.08200*.

Noah Shinn, Federico Cassano, Ashwin Gopinath, Karthik Narasimhan, and Shunyu Yao. 2023. Reflexion: Language agents with verbal reinforcement learning. *Advances in Neural Information Processing Systems*, 36:8634–8652.

Dong Shu, Xuansheng Wu, Haiyan Zhao, Daking Rai, Ziyu Yao, Ninghao Liu, and Mengnan Du. 2025. A survey on sparse autoencoders: Interpreting the internal mechanisms of large language models. *arXiv preprint arXiv:2503.05613*.

Karen Simonyan, Andrea Vedaldi, and Andrew Zisserman. 2014. Deep inside convolutional networks: Visualising image classification models and saliency maps. In *ICLR (Workshop Poster)*.

Daria Soboleva, Faisal Al-Khateeb, Robert Myers, Jacob R Steeves, Joel Hestness, and Nolan Dey. 2023. *SlimPajama: A 627B token cleaned and deduplicated version of RedPajama*. <https://www.cerebras.net/blog/slimpajama-a-627b-token-cleaned-and-deduplicated-version>

Samuel Soo, Wesley Teng, and Chandrasekaran Balaganesh. 2025. Steering large language models with feature guided activation additions. *arXiv preprint arXiv:2501.09929*.

Qwen Team. 2024. Qwq: Reflect deeply on the boundaries of the unknown. *Hugging Face*.

Adly Templeton. 2024. *Scaling monosemanticity: Extracting interpretable features from claude 3 sonnet*. Anthropic.

Ashish Vaswani, Noam Shazeer, Niki Parmar, Jakob Uszkoreit, Llion Jones, Aidan N Gomez, Łukasz Kaiser, and Illia Polosukhin. 2017. *Attention is all you need*. In *Advances in neural information processing systems*, pages 5998–6008.

Xuezhi Wang, Jason Wei, Dale Schuurmans, Quoc Le, Ed Chi, Sharan Narang, Aakanksha Chowdhery, and Denny Zhou. 2022. Self-consistency improves chain of thought reasoning in language models. *arXiv preprint arXiv:2203.11171*.

Jason Wei, Xuezhi Wang, Dale Schuurmans, Maarten Bosma, Fei Xia, Ed Chi, Quoc V Le, Denny Zhou, and 1 others. 2022. Chain-of-thought prompting elicits reasoning in large language models. *Advances in neural information processing systems*, 35:24824–24837.

Hanqi Yan, Yanzheng Xiang, Guangyi Chen, Yifei Wang, Lin Gui, and Yulan He. 2024. Encourage or inhibit monosemanticity? revisiting monosemanticity from a feature decorrelation perspective. *arXiv:2406.17969*.

Mingxi Zhang, Xuemin Li, Shuibo Yue, and Liuqian Yang. 2020. An empirical study of textrank for keyword extraction. *IEEE access*, 8:178849–178858.

Lianmin Zheng, Wei-Lin Chiang, Ying Sheng, Tianle Li, Siyuan Zhuang, Zhanghao Wu, Yonghao Zhuang, Zhuohan Li, Zi Lin, Eric. P Xing, Joseph E. Gonzalez, Ion Stoica, and Hao Zhang. 2023. [Lmsys-chat1m: A large-scale real-world llm conversation dataset](#). *Preprint*, arXiv:2309.11998.

A ReasonScore Details

A.1 Reasoning Vocabulary

In Fig. 5, we show the complete list of words from the *reasoning* vocabulary \mathcal{R} that we obtain in Sec. 3.1. For clarity, we list only the lowercase forms without spaces (e.g. “alternatively”). However, in our implementation, we track multiple forms of each word, including capitalized (“Alternatively”) and space-prefixed variants (“ alternatively”, “ Alternatively”), as the tokenizer can assign different tokens for each of the forms.

Our vocabulary includes several words that require additional clarification. Concretely, we retain “but” despite exceeding the frequency threshold, as a strong reasoning indicator, as shown in prior research. Empirical analysis further confirmed its association with reasoning transitions. We include “let me” as a phrase rather than “let” alone, since model consistently pair these tokens as a single reasoning unit. For “but” and “another”, we use only capitalized forms, as lowercase variants appear predominantly in non-reasoning contexts while capitalized forms mark reasoning transitions.

["alternatively", "hmm", "maybe", "wait", "perhaps", "let me", "therefore", "however", "but", "another"]

Figure 5: The complete list of words from the *reasoning* vocabulary \mathcal{R} in the lowercase and without spaces form.

A.2 Importance of Reasoning Words

To address whether our selected reasoning words truly reflect model’s reasoning capabilities or merely act as superficial linguistic markers, we conduct an ablation study that measures the importance of the reasoning vocabulary on model performance. Specifically, during the model generation, we **ban** words from our reasoning vocabulary so the model can’t output them during its thinking process. We then measure the performance of this setup using pass@1 metric on AIME-2024, MATH-500, and GPQA Diamond. To isolate the impact of reasoning words from the general effect of banning any words, we conducted an additional experiment where we banned an equal number of words, with each word *randomly* sampled from the p_{think} distribution (Sec. 3.1). For the *random words* experiment, we repeat it 10 times with different sets of words and report average pass@1.

Word-ban	AIME 2024		MATH-500		GPQA Diamond	
	pass@1	tokens (K)	pass@1	tokens (K)	pass@1	tokens (K)
Default	53.3	12.4	93.2	3.9	50.0	7.9
Reason	20.0	9.1	86.6	2.5	41.9	5.7
Random	48.6	13.3	89.4	4.2	48.5	8.9

Table 2: Performance and average number of output tokens (K) under word-ban experiments. **Default**: no banned words; **Reason**: ban the reasoning vocabulary; **Random**: ban random words.

The results, presented in Tab. 2, demonstrate that banning *reasoning* words significantly decreases both the performance and the reasoning depth (average number of output tokens). In contrast, banning random words produces no statistically significant differences from the baseline. This provides empirical evidence that these reasoning words play a functional role in the model’s reasoning process.

A.3 ReasonScore Distribution

Fig. 6 shows the ReasonScore values sorted in decreasing order of all SAE features for DEEPSEEK-R1-LLAMA-8B. We select the 0.997-th quantile as a cutoff, yielding approximately 200 features. While the plot shows the ReasonScore continues to decay below this threshold rather than reaching a plateau, this amount is feasible to analyze manually and contains all the most important features as judged by our metric.

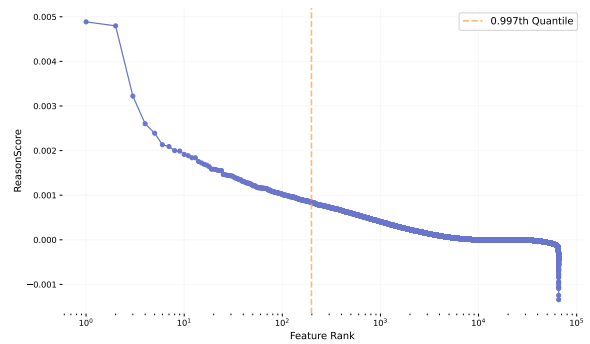


Figure 6: Distribution of ReasonScore values across all SAE features for DEEPSEEK-R1-LLAMA-8B, sorted in decreasing order.

B Interpretability Details

B.1 Feature Interfaces

Figs. 8,9 display additional activation patterns for features we found during manual interpretation (Sec. 4.2), highlighting tokens where each feature most strongly activates.

B.2 Automatic Interpretation Details

To interpret each feature, we randomly selected 30 examples from the OPENTHOUGHTS-114K dataset. The selection was stratified across different domains to ensure a balanced representation of various reasoning types and application contexts. The automatic feature interpretation followed a two-step pipeline. First, we used GPT-4O to generate free-form descriptions of the inferred function of each feature. This step involved detailed prompting, requesting the model to explain what the feature likely encodes and provide supporting examples.

After generating individual descriptions, we cluster reasoning-related features based on their possible functions and behavioral patterns. To support this process, we provided GPT-4O with a list of existing features, accompanied by a description of its possible function and observed steering behavior. The model was asked to identify recurring patterns and group similar features accordingly. To ensure accuracy, the results were then manually reviewed and validated. Table 4 presents the resulting feature groups, including categories (reasoning depth and thoroughness, self-correction and backtracking, and others), along with descriptions of their roles and effects. In some cases, even features grouped together based on shared function exhibited subtle differences in how they influenced responses; for instance, among features encouraging structural organization, one may focus on logical flow and paragraphing, while another influences transitions between argument steps. Additionally, features often demonstrated overlapping effects with other groups or influenced aspects beyond reasoning alone. For example, affecting the stylistic tone or structure of the output. This suggests that certain features may play a broader role across different types of reasoning and expression, rather than being confined to a single function.

C Examples of Feature Steering

Tab. 5 show the example of model’s thinking process on a “how many r’s in the word strawberry” question with and without steering. Tabs. 6,7,8 show the examples of model’s thinking processes on reasoning-related benchmarks with and without steering.

Layer	Reasoning Features			Random Features		
	diff	maybe	same	diff	maybe	same
13	52.5	14.0	33.5	76.0	9.0	15.0
15	43.5	17.0	39.5	63.0	13.0	24.0
17	27.0	17.0	56.0	49.0	13.0	38.0
21	17.5	23.5	59.0	50.0	9.0	41.0
23	17.5	22.0	60.5	54.0	15.0	31.0

Table 3: Cross-layer matching results for reasoning features and 100 random features from layer 19-th SAE. All values are in percentages (%).

D Generalization Experiments

D.1 Reasoning Capabilities Across Layers

We perform additional experiments by analyzing the existence of similar *reasoning* features across layers. We train multiple SAEs on activations from layers $\{13, 15, 17, 21, 23\}$ of the DEEPSEEK-R1-LLAMA-8B model. To match the features between different SAEs, we use the approach proposed in (Balagansky et al., 2024). For each layer, we match all features from our original 19-th layer SAE with all features in the considered layer. Formally, we aim to find a permutation matrix that aligns the features of layer A with those of layer B . This is done by minimizing the MSE between the decoder weights:

$$\begin{aligned} P^{(A \rightarrow B)} &= \arg \min_P \sum_{i=1}^n \|W_{\text{dec},i}^{(A)} - PW_{\text{dec},i}^{(B)}\|^2 \\ &= \arg \max_P \langle P, (W_{\text{dec}}^{(A)})^T W_{\text{dec}}^{(B)} \rangle_F. \end{aligned} \quad (8)$$

After matching each i -th feature from layer 19 with some other j -th SAE feature from a different layer, we take the subset corresponding to *reasoning* features (\mathcal{F}_R) and their corresponding matched subset. We evaluate the similarity of a pair of matched features (i, j) using a *Matching Score*, which is defined as the cosine similarity between feature activations across a batch of samples from OPENTHOUGHTS-114K:

$$\text{MS}(i, j) = \frac{\sum_{x \in D} f_i(x) \cdot f_j(x)}{\sqrt{\sum_{x \in D} f_i^2(x)} \cdot \sqrt{\sum_{x \in D} f_j^2(x)}}. \quad (9)$$

Here, D is a subset of token activations from OPENTHOUGHTS-114K, $|D| = 10M$ tokens.

We consider i -th reasoning feature to be presented in another layer as j -th feature if $\text{MS}(i, j) > 0.7$ (**same**), undefined if $0.5 < \text{MS}(i, j) \leq 0.7$ (**maybe**), and absent if $\text{MS}(i, j) \leq 0.5$ (**diff**).

```

Feature #19371
, output NO.\n\nBut how to efficiently implement this.\n\n
Return moving_avg\n\nBut what if the CSV has different
to the count.\n\nBut how to compute the intersection.\n\n
get the count.\n\nBut how to build these hash maps

Feature #4646
more.\n\nAlternatively, maybe there's a non-symmetric
insight.\n\nWait, maybe I need to assume that the
n.\n\nWait, maybe there's a different way to
als are perpendicular, maybe there's a simpler formula.

Feature #13448
is considered known. But maybe in the context of the
format, it's possible that the expected answer is \
No}.\n\nAlternatively, maybe the problem expects the answer
problem seems more elementary, maybe expecting Riemann.\n\n

Feature #46772
value.\n\nWait, perhaps we can think of the total
structure.\n\nWait, perhaps we can find that the updates
problem.\n\nWait, perhaps the minimal sum is not achieved
enough.\n\nAlternatively, perhaps we can use a heap,

```

Figure 7: Top-activating examples from the manually verified set of Nemotron features.

We present the results in Tab. 3, along with the matching scores for the 100 randomly sampled features from 19-th layer SAE to establish a baseline for comparison. Our analysis reveals that similar reasoning features exist across model layers (as judged by the *Matching Score*). For example, 39.5% of the features from layer 19 have close matches ($MS > 0.7$) in layer 15, significantly higher than the 24.0% matching rate for randomly chosen features.

D.2 Reasoning Capabilities Across Architectures

We train the SAE on the 19-th layer of a widely adopted open-source family of reasoning models, Nemotron (Bercovich et al., 2025). Specifically, we use the LLAMA-3.1-NEMOTRON-NANO-8B-v1 model and utilize its original training dataset to train our SAE. Otherwise, we follow the same experimental setup as in Sec. 4.1 of the main paper. We compute the ReasonScore for all features and select the top-200 as judged by the ReasonScore.

Following Sec. 4.2 of the main paper, we perform a manual interpretation of these features. We find the Nemotron features that have activation patterns similar to the ones in the DEEPSEEK-R1-LLAMA-8B model. In Fig. 7, we provide interfaces of features representing model's uncertainty (#46772), exploration (#13448), and reflection (#4646, #19371). These results indicate that reasoning features emerge across distinct families of reasoning LLMs.

Feature #16778
a lower concentration? Wait, but the initial thought was possible of them. Wait, no. Wait, the smallest possible. \n\nWait, let's think of it number. Wait, no, let's compute that again

Feature #31052
a perfect fit. But I'm not confident. Alternatively it's fit better. But I'm really not sure. the answer. \n\nBut I'm not entirely sure. Another conquer enemy, but I'm not certain. Alternatively,

Feature #43828
 a_{i+1} . \n\nBut this is unclear. \n\nAlternatively $+1=42$. But this is speculative. \n\nAlternatively of that intersection point. But this seems too abstract. \n\n $*4+3$. But this is just a guess

Feature #45699
a bit of a dilemma. \n\nWait, let me This is a bit ambiguous. To avoid confusion, I perspective, disputes might be. \n\nBut without context, the So there's a conflict. To resolve this, perhaps

(a) Top-activating examples from the manually verified set of features. The chosen examples represent “uncertainty”.

Feature #40262
of a ship, but maybe “keel” relates coffin” could be a pun on “c ‘t make sense. Or maybe a homophone. “ I’m not sure. Alternatively, 500 in Roman numer

Feature #34967
think of possible groupings. \n\nAlternatively, maybe the groups is a guess. \n\nWait, maybe the user expects me a missing detail. Alternatively, maybe the pie chart was I’m not certain. Wait, the options are (A

Feature #1451
“exit.” \n\nWait, another angle: the room’s missed something. Let me think again. The standard electrode fit. \n\nWait, another thought: maybe the answer confusing. Wait, let me try another approach. The

Feature #33429
not the case. Alternatively, maybe the problem is expecting is known, so maybe the answer is simply -57. Alternatively, maybe the problem is testing the knowledge that \n\nWait, maybe the problem is a simple application of

(b) Top-activating examples from the manually verified set of features. The chosen examples represent “exploration”.

Figure 8: Examples of feature interfaces used in manual interpretation experiments.

Feature #506
barycentric coordinates... I think there's a enter can be given, but I might need to recall)\n\nBut this seems complicated. Alternatively, perhaps it's external angle bisectors. \n\nBut I'm not sure how

Feature #9636
P and Q. \n\nWait, but we have P(B be necessary for our problem. Let's return to the help with the inequality? \n\nWait, maybe use Cauch would take the triangle. \n\nBut the problem states that the

Feature #9977
of the rows. \n\nBut the problem states “any initial feasible. However, the problem states that N is presence of competitors. But the question specifically asks about temperature done after chlorination. But the question says

Feature #34370
seems straightforward. But let me verify with actual numbers to .\n\nWait, but let me double-check. The problem 1. But let me try another way to solve 3.\n\nWait, let me check my steps again to

(a) Top-activating examples from the manually verified set of features. The chosen examples represent “reflection”.

Feature #34431
is 530 J. \n\nBut another approach: 5 10⁴ g Å². \n\nBut maybe the calculation allows for be 17. However, sometimes when the first digit 1680 J. \n\nHowever, in our precise calculation,

Feature #54382
121 is the smallest. \n\nBut wait, let's check a mistake in the reasoning. \n\nWait, but the problem as R=4. Hmm. What about R= 's a different answer. \n\nWait, let's consider another

Feature #56769
or Poisson's ratio. This is a problem because it's not mentioned here. Hmm. The user might knowing the refractive index? Wait, maybe there's natural frequency without knowing E. Maybe there is a standard

Feature #57334
not likely. \n\nWait, perhaps I'm making a mistake already present. \n\nWait, perhaps the reaction uses a different substitution should be meta. Unless there's some steric does that happen? \n\nAlternatively, maybe the first Cl goes

(b) Top-activating examples from the manually verified set of features. The chosen examples represent mixed behaviors.

Figure 9: Examples of feature interfaces used in manual interpretation experiments.

Group Name	Features	Possible Function	Effect Type	Observed Behavior
Reasoning Depth and Thoroughness	506, 4395, 9636, 23052, 30288, 33148, 54382, 61935	Controls multi-step analysis, iteration, and self-correction in problem-solving.	Stylistic & Structural, Semantic & Logical Consistency	Strengthening: Extensive step-by-step reasoning, multiple iterations, self-corrections. Weakening: Direct answers with minimal steps.
Numerical Accuracy and Validation	4990, 3466, 16778, 46379, 34813, 51765	Governs precision in calculations, unit conversions, and error-checking.	Semantic & Logical Consistency	Strengthening: Meticulous unit tracking, iterative re-evaluation. Weakening: Direct results with potential errors.
Exploration of Multiple Methods	22708, 62446	Encourages evaluating alternative approaches before finalizing solutions.	Semantic & Logical Exploration	Strengthening: Compares multiple strategies (e.g., DP vs. greedy). Weakening: Commits to the first viable method.
Structural and Logical Organization	57334, 43828, 45699, 49326, 17726, 46449, 41636, 40262	Ensures clarity, step-by-step breakdown, and logical flow. It may also balance executable code generation vs. verbal explanations.	Structural, Semantic & Instruction Clarity	Strengthening: Well-structured explanations. Weakening: Disorganized or fragmented reasoning.
Symbolic vs. Numerical Reasoning	48026, 34967, 34589	Balances theoretical/symbolic reasoning with direct numerical computation.	Semantic & Logical Consistency	Strengthening: Algebraic/theoretical frameworks. Weakening: Immediate numerical substitution.
Self-Correction and Backtracking	16778, 35337, 42609, 34431, 25953	Controls iterative refinement and error-checking.	Semantic & Logical Consistency	Strengthening: Multiple rounds of self-correction. Weakening: Commits to initial answers without revision.
Causal Chaining & Scientific Context	56769, 34370, 3261, 13457	Enforces clear multi-step causal linkages in science/environmental scenarios, modulates temporal reasoning, hypothetical alternatives and scenario simulation	Semantic (Causality)	Strengthening: yields explicit causal chains, regulates contrastive reasoning, gives clearer timeline-based reasoning. Weakening: results in loosely linked assertions or missing intermediate steps, omit historical or causal context
Edge Case and Constraint Handling	16343, 46691, 3942	Ensures validation of edge cases and constraints.	Semantic & Logical Consistency	Strengthening: Explicitly addresses edge cases. Weakening: Assumes valid inputs without verification.
Semantic Elaboration & Conceptual Depth	1451, 33429, 61104, 25485, 45981, 31052, 16441, 53560	Shapes depth of domain-specific explanations, analogies, trade-off discussions, and interdisciplinary links	Semantic (Elaboration & Breadth)	Strengthening: Adds conceptual depth through analogies, trade-offs, and multi-factor explanations. Weakening: Reduces to simple, surface-level or single-cause statements with minimal abstraction.
Other Behavior	48792, 9977, 20046, 12036, 32134	Include: influences engagement and conversational tone, assertiveness/redundancy/structure in text and terminology	Stylistic & Structural	Strengthening: Creates a more formal, robotic style with rigid structure and a high degree of confidence in statements. Weakening: Makes the style livelier and more conversational, with informal delivery, varied structure, and a moderate level of confidence that includes elements of uncertainty and flexibility.

Table 4: Reasoning clusters obtained using GPT-4O. Each cluster is defined by a particular type of reasoning (depth of analysis, numerical checking, code generation), the specific features involved, their hypothesized function in shaping the models' output style and logic, and the observed behaviors that emerge when using the feature steering.

Problem: How many r's are in the word strawberry?

Generation (no steering): I need to determine how many times the letter "r" appears in the word "strawberry." First, I'll write down the word and break it into individual letters: S, T, R, A, W, B, E, R, R, Y. Next, I'll identify which of these letters are "r": the third, eighth, and ninth letters. Finally, I'll count these "r"s, which gives me a total of **three**.

Generation (steering): Okay, so I need to figure out how many r's are in the word "strawberry." Let me think about this step by step. First, I should probably write down the word and break it down into its individual letters. The word is spelled S-T-R-A-W-B-E-R-R-Y. Wait, let me make sure I have that right. Sometimes I get confused with the spelling. I think the correct spelling is "strawberry." So, let me write it out again: S, T, R, A, W, B, E, R, R, Y. Hmm, now that I write it, I see there are two R's after the E. Let me count the letters again to make sure I don't miss any. S (1), T (2), R (3), A (4), W (5), B (6), E (7), R (8), R (9), Y (10). So the word has 10 letters in total. Now, focusing on the R's. The third letter is R, that's one. Then after E, which is the seventh letter, there are two more R's: the eighth and ninth letters. So that's two more. Let me double-check the spelling again to make sure I'm not miscounting. Sometimes I might confuse the letters. I think it's S-T-R-A-W-B-E-R-R-Y, so yes, the two R's are towards the end. Wait, is there another R in the word? Let me think. The word is "strawberry." I think it's spelled with an R after the E, and another R after that. So that's two R's. I don't recall any other R's in the word. Let me go through each letter again: S, T, R, A, W, B, E, R, R, Y. So, yes, the R's are the third, eighth, and ninth letters. Wait, that's three R's. Did I miscount earlier? Wait, no, I think I made a mistake. Let me recount the letters with their positions. Let's write it out:

1. S
2. T
3. R
4. A
5. W
6. B
7. E
8. R
9. R
10. Y

So, the R's are at positions 3, 8, and 9. That makes three R's in total. I think I initially thought it was two, but upon a closer examination, it's actually three. Let me check another source or think about how the word is pronounced. The word "strawberry" is pronounced with a double R sound, so that would correspond to two R's, but when I break it down, I see that the letters are R, R. Wait, no, the letters are E, R, R. So, that's two R's after the E. So, the third letter is R, and then the eighth and ninth letters are R's as well. So that's three R's. Wait, I'm getting confused. Let me visualize the word again: S-T-R-A-W-B-E-R-R-Y. So, the letters are S, T, R, A, W, B, E, R, R, Y. So, the R appears at the third position, and then again at the eighth and ninth positions. That makes three R's. So, the correct count is three R's. I think I initially miscounted because I focused on the double R at the end, but there's another R earlier in the word. So, to clarify, the word "strawberry" has three R's: one in the third position, and two more at the end. So, the correct answer is **three** R's.

Table 5: An example of “How many r's are in the word strawberry?” problem and corresponding full outputs from DEEPSEEK-R1-LLAMA-8B and its steered version.

Problem: Tom got a Mr. Potato Head for his birthday. It came with 3 hairstyles, 2 sets of eyebrows, 1 pair of googly eyes, 2 sets of ears, and 2 sets of lips, a pair of regular shoes, and a bonus pair of clown shoes. If a complete Mr. Potato Head personality includes eyebrows, eyes, ears, lips, shoes and optionally hair, how many different wacky personalities can Tom come up with? Note that Mr. Potato Head can be bald. Note: You cannot "mix and match". For example, you cannot take the left eyebrow from one pair and the right eyebrow from the other pair.

Generation (no steering): First, I need to understand the components that make up a complete Mr. Potato Head personality. According to the problem, a personality includes eyebrows, eyes, ears, lips, shoes, and optionally hair. Additionally, Tom received various options for each of these components. Starting with the eyes, there is only one pair of googly eyes available. Since they must be used as a whole pair, there is only 1 way to choose the eyes. Next, the ears come in 2 sets. Each set represents a different style, so there are 2 possible choices for the ears. For the eyebrows, there are 2 sets available. Each set is used entirely, so there are 2 choices for the eyebrows. The lips also come in 2 sets, meaning there are 2 options for the lips. Shoes are either regular or clown shoes, and since both are complete pairs, there are 2 choices for the shoes. Hair is optional and includes 3 different hairstyles. Therefore, there are 3 choices for the hair, but it's not required to choose any.

Now, to calculate the total number of different personalities, I'll multiply the number of choices for each component. The eyes, ears, eyebrows, and lips each have 1, 2, 2, and 2 choices respectively. The shoes have 2 choices, and the optional hair adds 3 possibilities.

So, the total number of personalities is $1 \text{ (eyes)} \times 2 \text{ (ears)} \times 2 \text{ (eyebrows)} \times 2 \text{ (lips)} \times 2 \text{ (shoes)} \times 3 \text{ (hair)} = 24$ different personalities.

Generation (steering): Alright, so Tom got this Mr. Potato Head, and he wants to figure out how many different wacky personalities he can create. The problem gives a list of parts: 3 hairstyles, 2 sets of eyebrows, 1 pair of googly eyes, 2 sets of ears, 2 sets of lips, a pair of regular shoes, and a bonus pair of clown shoes. The key here is that a complete personality includes eyebrows, eyes, ears, lips, shoes, and optionally hair. Also, it's important to note that you can't mix and match parts; you have to use the entire pair or set as given. First, let me break down the components and see how they contribute to the total number of personalities. The problem mentions that some parts are optional, specifically the hairstyles. So, the personality can be bald, meaning the hairstyle part is optional. Let's list out all the components:

1. Hairstyles: 3 options. These can be considered optional since the problem states that Mr. Potato Head can be bald.
2. Eyebrows: 2 sets. Since both eyes and eyebrows are required, we have to choose one set of eyebrows. So, there are 2 choices here.
3. Eyes: 1 pair of googly eyes. It seems like there's only one option here because it's just a single pair. So, eyes are required, and there's only one choice for them.
4. Ears: 2 sets. Similar to eyebrows, we have to choose one set of ears, so that's 2 choices.
5. Lips: 2 sets. Again, choosing one set, so 2 choices.
6. Shoes: 2 types (regular and clown). Since shoes are required, we have two options here.

Now, let's structure this. The components that are required are eyes, eyebrows, ears, lips, and shoes. The optional component is the hairstyle. Since the hairstyles can be chosen or not, that adds some flexibility. So, let's calculate the number of options for each required component: Eyebrows: 2 options, Eyes: 1 option, Ears: 2 options, Lips: 2 options, Shoes: 2 options. Multiplying these together gives us the number of ways to choose the required components: $2 \times 1 \times 2 \times 2 \times 2$. Calculating that: 2×1 is 2, times 2 is 4, times 2 is 8, times 2 is 16. So, there are 16 ways to choose the required components.

Now, considering the optional hairstyle. Since there are 3 hairstyles and the Mr. Potato Head can be bald, that means for each combination of the required parts, there are 4 possible choices (including the option of no hairstyle). Wait, hold on, actually, the problem says that the complete personality includes eyebrows, eyes, ears, lips, shoes, and optionally hair. So, does that mean that the hair is optional on top of the required parts? So, for each required component setup, we can choose one of the 3 hairstyles or choose to be bald. Hmm, does being bald count as a separate option, or is it just not using any hairstyle? Wait, the problem says "you cannot 'mix and match'", but that's about using entire sets, not about the hairstyle. So, if the problem allows being bald, that's a fourth option for the hairstyle. Therefore, the number of choices for the hairstyle is 4.

So, now, the total number of personalities would be the number of ways to choose the required components multiplied by the number of choices for the hairstyle. Earlier, we found that the required components can be arranged in 16 ways. For each of these 16 ways, we can choose one of the 4 hairstyles (including bald). So, that would be 16×4 . Calculating that: 16×4 is 64.

But let me think again. Is the pair of regular shoes considered as 1 option or 2? Wait, the problem says a pair of regular shoes and a bonus pair of clown shoes. So, the shoes are either regular or clown. So, that's two options, right? So, that's 2 choices for shoes. So, that seems correct. So, summarizing:

Eyebrows: 2, Eyes: 1, Ears: 2, Lips: 2, Shoes: 2. Multiply those: $2 \times 1 \times 2 \times 2 \times 2 = 16$. Hair: 3 + 1 (bald) = 4.

Total: $16 \times 4 = 64$. Therefore, the total number of different wacky personalities Tom can come up with is 64.

Wait, just to make sure, is there any possibility that the problem is considering the shoes as a separate category? Let me check the problem again. It says: "a pair of regular shoes, and a bonus pair of clown shoes." So, that's two different shoes: regular and clown. So, the shoes are either regular or clown, so two options. Therefore, the shoes contribute 2 to the total, which we included. So, the calculations are correct. Therefore, the final answer is 64.

Table 6: A problem from MATH-500, and corresponding outputs from DEEPSEEK-R1-LLAMA-8B and its steered version. Correct answer: 64.

Problem: A regular octagon has the same perimeter as the regular hexagon shown here with side length 16 cm. How long is each side of the octagon? [asy]size(80); pair A = dir(120); pair B=dir(60); pair M=(A+B)/2; draw(dir(360)-B-A-dir(180)-dir(240)-dir(300)-cycle); label("16 cm", M, N);[/asy]

Generation (no steering): Okay, so I have this problem where a regular octagon has the same perimeter as a regular hexagon. The hexagon has a side length of 16 cm, and I need to find the side length of the octagon. Hmm, let's break this down step by step. First, I remember that the perimeter of a regular polygon is just the number of sides multiplied by the length of each side. So, for the hexagon, which is a six-sided polygon, I can calculate its perimeter by multiplying 6 by 16 cm. Let me write that out:

$$\text{Perimeter of hexagon} = 6 * 16 \text{ cm} = 96 \text{ cm.}$$

Got that. So the perimeter of the octagon must also be 96 cm since it's equal to the hexagon's perimeter. Now, a regular octagon has 8 sides, right? So, if I let 's' be the length of each side of the octagon, then the perimeter of the octagon would be $8 * s$. Since we know the perimeter is 96 cm, I can set up the equation:

$$8 * s = 96 \text{ cm.}$$

To find 's', I just need to divide both sides by 8:

$$s = 96 \text{ cm} / 8 = 12 \text{ cm.}$$

Wait, is that it? It seems straightforward, but let me double-check to make sure I didn't miss anything. So, the hexagon has 6 sides, each 16 cm, so $6 * 16 = 96$ cm. The octagon has 8 sides, so each side is $96/8=12$ cm. Yep, that seems correct. Hmm, just to make sure, maybe I should visualize the polygons. A regular hexagon has six equal sides and six equal angles, and a regular octagon has eight equal sides and eight equal angles. Since both are regular, all sides and angles are equal, so the calculation should hold.

Another way to think about it: the perimeter is just the sum of all sides. So, for the hexagon, adding up six sides each of 16 cm gives 96 cm. For the octagon, we need to add up eight sides, each of which is the same length, so 8 times that length equals 96 cm. Solving for that length gives 12 cm. I don't see any mistakes in the logic here. It's a direct calculation based on the definition of perimeter for regular polygons. So, I think the side length of the octagon is 12 cm.

Final Answer

The length of each side of the octagon is 12 centimeters.

Generation (steering): Okay, so I have this problem here where I need to figure out the length of each side of a regular octagon. The octagon has the same perimeter as a regular hexagon, and the hexagon is shown with side length 16 cm. Hmm, okay, let me think step by step about how to approach this. First, I remember that the perimeter of a shape is the total length around it. For regular polygons, which both octagons and hexagons are, the perimeter is just the number of sides multiplied by the length of each side. So if I can figure out how many sides each shape has and then use the given information, I can find the opposite. Wait, the problem says it's a regular hexagon. Right, a hexagon has six sides. So, since the side length is 16 cm, the perimeter of the hexagon would be 6 times 16 cm. Let me write that down.

$$\text{Perimeter of hexagon} = 6 * 16 \text{ cm} = 96 \text{ cm.}$$

So, the octagon has the same perimeter, which is 96 cm. Now, an octagon has eight sides. So, if I can find the length of each side of the octagon, that would be the perimeter divided by 8. Let me write that formula:

$$\text{Perimeter of octagon} = 8 * (\text{length of each side})$$

But wait, we know the perimeter is 96 cm, so:

$$96 \text{ cm} = 8 * (\text{length of each side})$$

To find the length of each side, I need to divide both sides by 8. So, length of each side = $96 \text{ cm} / 8 = 12 \text{ cm}$. Hmm, that seems straightforward. But let me just double-check to make sure I didn't make a mistake. Wait, is it correct that the octagon's perimeter is 96 cm? Because the hexagon's side is 16 cm, so 6 times 16 is 96. So, yes, the octagon has to have the same perimeter. Since octagons have more sides, each side should be shorter. So, 96 divided by 8 is 12, which is shorter than 16, so that makes sense. Wait, another way to think about it: if you have a polygon with more sides, each side is actually shorter for the same perimeter. So, since an octagon has more sides than a hexagon, each side should be shorter, which aligns with 12 cm being shorter than 16 cm. So that seems right. Is there another way to approach this problem? Maybe using the formula for perimeter in terms of side length? Yes, for regular polygons, the perimeter is just the number of sides multiplied by the side length. So, if I denote the side length of the octagon as 's', then:

$$\text{Perimeter of octagon} = 8 * s$$

But since it's equal to the perimeter of the hexagon, which is $6 * 16 = 96$, then: $8s = 96$ Solving for s gives $s = 96 / 8 = 12 \text{ cm}$. Yep, same result. I think I got it. So, the length of each side of the octagon is 12 cm. Wait, let me think again. Sometimes, when I'm dealing with perimeters, I might confuse side length with something else, but in this case, since both are regular polygons, it's straightforward. So, for regular polygons, the perimeter is directly additive. So, each side contributes equally. Therefore, inverting the number of sides inversely affects the side length. So, in the hexagon, 6 sides, each 16 cm, so 16 times 6 is 96. The octagon, which has more sides, 8, so each side is 96 divided by 8, which is 12. So, that makes sense. Wait, just to make sure, if the octagon had 8 sides, each 12 cm, the perimeter would be $8 * 12 = 96 \text{ cm}$, which is the same as the hexagon. So, that's correct. I think that's solid. So, the length of each side of the octagon is 12 cm.

Final Answer

The length of each side of the octagon is 12 cm.

Table 7: A problem from MATH-500, and corresponding outputs from DEEPSEEK-R1-LLAMA-8B and its steered version. Correct answer: 12 cm.

Problem: Remmy wants to divide 10 by $\frac{2}{3}$, but he cannot remember how to do that. By what number should he multiply 10 to get the answer?

Generation (no steering): Okay, so Remmy has this problem where he needs to divide 10 by $\frac{2}{3}$, but he's forgotten how to do division with fractions. Hmm, I remember that dividing by a fraction is the same as multiplying by its reciprocal, but let me think through it step by step to make sure I get it right. First, division. If we have a division problem like 10 divided by something, in this case, 10 divided by $\frac{2}{3}$, the basic idea is to find out how many times $\frac{2}{3}$ fits into 10. But when dealing with fractions, it can get a bit tricky, so maybe breaking it down will help. I recall that dividing by a fraction is equivalent to multiplying by its reciprocal. The reciprocal of a fraction is just flipping the numerator and denominator. So, the reciprocal of $\frac{2}{3}$ is $\frac{3}{2}$. That means 10 divided by $\frac{2}{3}$ is the same as 10 multiplied by $\frac{3}{2}$. Let me write that out: $10 \div (\frac{2}{3}) = 10 \times (\frac{3}{2})$

Okay, so now I just need to compute 10 multiplied by $\frac{3}{2}$. To do that, I can think of 10 as a fraction, which is $\frac{10}{1}$. Then, multiplying two fractions is straightforward: multiply the numerators and the denominators. So, $\frac{10}{1} \times \frac{3}{2} = (\frac{10 \times 3}{1 \times 2}) = \frac{30}{2}$. Hmm, 30 divided by 2 is 15. So, 10 divided by $\frac{2}{3}$ is 15. That makes sense because $\frac{2}{3}$ is less than 1, so dividing by a number less than 1 should give a result larger than the original number.

Wait, let me double-check that. If I have $\frac{2}{3}$, how many times does it go into 10? Well, $\frac{2}{3}$ times 15 should be 10. Let me verify that: $(\frac{2}{3}) \times 15 = (2 \times 15)/3 = 30/3 = 10$. Yes, that's correct. So, 15 is the right answer.

Alternatively, maybe I can think about this in another way to confirm. If I have 10 divided by $\frac{2}{3}$, it's like asking how much do I have to multiply $\frac{2}{3}$ by to get 10. So, if I set it up as an equation: $(\frac{2}{3}) \times x = 10$. To solve for x, I can multiply both sides by the reciprocal of $\frac{2}{3}$, which is $\frac{3}{2}$: $x = 10 \times (\frac{3}{2}) = 15$. Same result. That seems consistent.

Another way to think about division with fractions is by using decimals. $\frac{2}{3}$ as a decimal is approximately 0.6667. So, if I divide 10 by 0.6667, what do I get? Let me calculate that. $10 \div 0.6667$ is approximately 15.0. That matches the previous answers, so that's good. Hmm, so all methods lead me to 15. That must be the correct answer. Just to recap: Dividing by a fraction is the same as multiplying by its reciprocal; The reciprocal of $\frac{2}{3}$ is $\frac{3}{2}$; $10 \times \frac{3}{2} = 30/2 = 15$; Verification by multiplying $\frac{2}{3}$ by 15 gives back 10; Converting to decimals also gives 15. Therefore, I'm confident that the answer is 15.

Final Answer The number Remmy should multiply 10 by is 15.

Generation (steering): Okay, so Remmy wants to divide 10 by $\frac{2}{3}$, but he's a bit fuzzy on how to do that. Hmm, I remember that dividing by a fraction is the same as multiplying by its reciprocal. Let me think if that's right. So, if you have something like 10 divided by $\frac{2}{3}$, it should be the same as 10 multiplied by $\frac{3}{2}$. Yeah, that sounds familiar from what I've learned before.

Wait, let me make sure I'm not mixing things up. Sometimes, when you see division, you might be tempted to think of it as subtracting, but no, division is more about finding how many times one number fits into another. So, when you divide by a fraction, you're actually scaling up the original number because the divisor is less than 1. That makes sense because $\frac{2}{3}$ is less than 1, so dividing by it should give a larger result than 10. Let me break it down step by step. The problem is 10 divided by $\frac{2}{3}$. To make it clearer, I can write that as $10 \div (\frac{2}{3})$. Now, dividing by a fraction is equivalent to multiplying by its reciprocal. The reciprocal of $\frac{2}{3}$ is $\frac{3}{2}$, right? So, if I flip the divisor, it becomes $\frac{3}{2}$. So, now the problem becomes 10 multiplied by $\frac{3}{2}$. Let me compute that. 10 times 3 is 30, and 30 divided by 2 is 15. So, the result of 10 divided by $\frac{2}{3}$ is 15.

But wait, the question isn't asking for the answer itself; it's asking by what number Remmy should multiply 10 to get the answer. So, in this case, it's $\frac{3}{2}$. Hold on, let me verify that again. If I have 10 and I multiply it by $\frac{3}{2}$, I get 15, which is indeed the result of dividing 10 by $\frac{2}{3}$. So, yes, $\frac{3}{2}$ is the correct multiplier. Alternatively, I can think of it as 10 multiplied by 1.5, which is also 15. So, both ways, it checks out. Is there another way to approach this problem? Maybe by converting the division into a multiplication problem from the start. So, instead of $10 \div (\frac{2}{3})$, I can rewrite this as 10 multiplied by the reciprocal of $\frac{2}{3}$, which is $\frac{3}{2}$. That again gives me 15 when I do the multiplication. So, that's consistent.

I wonder if I can visualize this. If I have 10 wholes and I want to divide them into portions of $\frac{2}{3}$ each, how many portions would I have? Well, each portion is $\frac{2}{3}$, so to get 10 portions, I need to figure out how much each portion is. But wait, that's the opposite. Maybe that's confusing. Let me think differently. Suppose I have 10 cookies, and each cookie is cut into 3 equal pieces. Each piece would be $\frac{1}{3}$ of a cookie. But if I don't cut them all the way, maybe I cut each cookie into $\frac{2}{3}$ pieces. Hmm, not sure if that helps. Alternatively, if I have 10 apples and I want to distribute them among $\frac{2}{3}$ of a basket each, how many baskets would I need? But maybe that's overcomplicating it.

Perhaps it's better to stick with the mathematical approach. So, 10 divided by $\frac{2}{3}$ is the same as 10 times $\frac{3}{2}$, which is 15. Therefore, Remmy should multiply 10 by $\frac{3}{2}$ to get the answer.

Let me also think about the properties of division and multiplication. Division can be seen as the inverse operation of multiplication. So, if you have $a \div (b/c)$, it's equivalent to $a \times (c/b)$. Applying that here, $10 \div (\frac{2}{3})$ is $10 \times (\frac{3}{2})$. Yep, that's exactly what I did earlier. Just to make sure I haven't made any calculation errors, let me do the multiplication again. 10 times 3 is 30, and 30 divided by 2 is 15. So, 10 times $\frac{3}{2}$ is 15. That seems right. Alternatively, if I think about decimals, $\frac{2}{3}$ is approximately 0.6667. So, 10 divided by 0.6667 should be roughly 15. Let me compute that. 10 divided by 0.6667. Well, 0.6667 goes into 10 about 15 times because 0.6667 times 15 is 10. That's a good check. I think I'm confident now that the number Remmy should multiply 10 by is $\frac{3}{2}$. So, $\frac{3}{2}$ is the correct multiplier.

Final Answer Remmy should multiply 10 by 3/2.

Table 8: A problem from MATH-500, and corresponding outputs from DEEPSEEK-R1-LLAMA-8B and its steered version. Correct answer: 3/2.

Problem: A curve is parameterized by $(x, y) = (t^3 + 7, -3t^2 - 6t - 5)$.

Find the point the curve passes through at $t = 2$.

Generation (no steering): Okay, so I have this problem here where a curve is parameterized by the equations $x = t^3 + 7$ and $y = -3t^2 - 6t - 5$. I need to find the point the curve passes through when $t = 2$. Hmm, let me think about how to approach this. First, I remember that when you have a parameterized curve, each value of t corresponds to a specific point (x, y) on the curve. So, to find the point when $t = 2$, I just need to substitute $t = 2$ into both the equations for x and y and compute the values. That makes sense because each parameter t defines a unique point on the curve. Alright, let's start with the equation for x . The equation is $x = t^3 + 7$. So, substituting $t = 2$ into this should give me the x -coordinate of the point. Let me compute that step by step. Calculating t^3 when $t = 2$: $2^3 = 8$. Then, adding 7 to that: $8 + 7 = 15$. So, the x -coordinate is 15. That seems straightforward. Now, moving on to the y -coordinate. The equation is $y = -3t^2 - 6t - 5$. Again, substituting $t = 2$ into this equation. Let me break it down. First, compute t^2 when $t = 2$: $2^2 = 4$. Then, multiply that by -3 : $-3 \times 4 = -12$. Next, compute $-6t$ when $t = 2$: $-6 \times 2 = -12$. Lastly, we have the constant term, which is -5 . So, putting it all together: $y = (-12) + (-12) + (-5)$. Wait, hold on. Let me double-check that. The equation is $y = -3t^2 - 6t - 5$. So, substituting $t = 2$, it's $-3 \times (2)^2 - 6 \times (2) - 5$. That is $-3 \times 4 - 12 - 5$. So, $-12 - 12 - 5$. Adding those together: $-12 - 12$ is -24 , and $-24 - 5$ is -29 . So, the y -coordinate is -29 . Let me make sure I did that correctly. So, $-3 \times (2)^2$ is $-3 \times 4 = -12$. Then, -6×2 is -12 , and then subtracting 5. So, adding all those up: $-12 - 12$ is -24 , minus another 5 is -29 . Yeah, that seems right. So, combining both coordinates, when $t = 2$, the point on the curve is $(15, -29)$. Hmm, let me just verify once more in case I made any calculation errors. Starting with x : $t^3 + 7$. $t = 2$, so 2^3 is 8, plus 7 is 15. That's correct. For y : $-3t^2 - 6t - 5$. $t = 2$: $-3 \times (4) = -12$, $-6 \times 2 = -12$, and the constant is -5 . So, adding them: $-12 - 12$ is -24 , minus 5 is -29 . That's correct. Okay, so I think that's the point. Just to visualize, when $t = 2$, the curve is at $(15, -29)$. I don't see any mistakes in my calculations, so I feel confident about this answer.

Final Answer
The point the curve passes through at $t = 2$ is $(15, -29)$.

Generation (steering): Alright, so I have this problem here where a curve is parameterized by the equations $x = t^3 + 7$ and $y = -3t^2 - 6t - 5$. I need to find the point the curve passes through when $t = 2$. Hmm, okay, let me think about how to approach this. First, I remember that parameterized equations give both the x and y coordinates in terms of a third variable, which in this case is t . So, when they ask for the point when $t = 2$, I need to substitute $t = 2$ into both equations for x and y and then find the corresponding (x, y) pair. Let me write that down step by step. So, for x , the equation is $x = t^3 + 7$. If I plug in $t = 2$, that should give me the x -coordinate. Similarly, for y , the equation is $y = -3t^2 - 6t - 5$, so substituting $t = 2$ there should give me the y -coordinate. Once I have both values, I can combine them into a point. Okay, let me start with calculating x . Plugging $t = 2$ into $x = t^3 + 7$:

$$x = (2)^3 + 7.$$

Calculating 2^3 , that's 8, right? So, $8 + 7$ is 15. So, the x -coordinate when $t = 2$ is 15. That seems straightforward. Now, moving on to the y -coordinate. The equation is $y = -3t^2 - 6t - 5$. Plugging in $t = 2$: $y = -3(2)^2 - 6(2) - 5$.

Let me compute each term step by step. First, 2^2 is 4, so multiplying that by -3 gives -12 . Next, 6×2 is 12, so with the negative sign, that term becomes -12 . Then, the last term is just -5 . So, putting it all together: $-12 - 12 - 5$. Let's add those numbers. $-12 - 12$ is -24 , and then subtracting another 5 gives -29 . So, the y -coordinate is -29 . Wait, let me double-check that calculation because sometimes when I have multiple negative signs, I might mix them up. So, let me recast it:

$$y = -3(4) - 6(2) - 5.$$

That's $-12 - 12 - 5$. Yes, that's correct. $-12 - 12$ is indeed -24 , and $-24 - 5$ is -29 . So, that seems right. So, to recap, when $t = 2$, the x -coordinate is 15 and the y -coordinate is -29 . Therefore, the point the curve passes through is $(15, -29)$. Wait, just to make sure I didn't make a mistake in the substitution, let me verify each step again. For x , substituting $t = 2$ into $t^3 + 7$: $2^3 = 8$, so $8 + 7 = 15$. That's correct. For y , substituting $t = 2$ into $-3t^2 - 6t - 5$:

$$\text{First term: } -3 \times (2)^2 = -3 \times 4 = -12.$$

$$\text{Second term: } -6 \times 2 = -12.$$

$$\text{Third term: } -5.$$

Adding them up: $-12 - 12 - 5 = (-12 - 12) - 5 = -24 - 5 = -29$. Yep, that's correct. Hmm, I think that's solid. Maybe I should just think about whether the parameterization makes sense or if there's another way to represent this curve. Wait, actually, I might recall that sometimes parameterizations can be tricky, but in this case, it's pretty straightforward. It's giving x and y in terms of t , so plugging in $t=2$ should give the point. Alternatively, I can also compute the values for $t=2$ in both equations and plot them mentally or on paper. Let me sketch a rough graph in my mind. So, when $t=2$, x is 15, which is further out on the x -axis, and y is -29 , which is quite low on the y -axis. That seems plausible for a cubic and quadratic parameterization. Wait, another thought: sometimes, when I parameterize, especially with higher powers, I might have to check for consistency, but in this case, since both x and y are given, and the question is just about plugging in a specific t , I think it's safe. So, to sum up, substituting $t=2$ into both equations gives $x=15$ and $y=-29$, so the point is $(15, -29)$. I think that's the correct answer.

Final Answer
The point the curve passes through at $t = 2$ is $(15, -29)$.

Table 9: A problem from MATH-500, and corresponding outputs from DEEPSEEK-R1-LLAMA-8B and its steered version. Correct answer: $(15, -29)$.